DRA

THE METEOROID ENVIRONMENT OF PROJECT APOLLO

January 31, 1963

THE METEOROID ENVIRONMENT OF PROJECT APOLLO

January 31, 1963

By G. T. Orrok

Bellcomm, Inc.
Washington, D.C.

TABLE OF CONTENTS

PURPOSE AND SCOPE

To discuss the meteoroid hazard to the currently conceived Apollo mission, a knowledge of three factors is required.

These are (1) the potential hazard offered by the environment, (2) the susceptibility of the spacecraft as indicated by its detailed design, and (3) the allowable hazard, as governed by considerations of over-all system reliability.

The scope of this document is restricted to the first factor.

ABSTRACT

The meteoroid hazard to the Apollo mission is reviewed. A model for engineering design purposes is presented. The principal assumptions are a Watson-style flux magnitude plot, the Charters and Locke penetration criterion, a meteoroid density of 0.5 gm/cc, and a mass of 2.5 grams for a zero magnitude meteor of velocity 30 km/sec. After analysis of available data, it is estimated that the solid skin thickness required for protection to a given impact probability is known to a factor of about 2.5 times.

The erosion rate in deep space is estimated as 10-20 angstrom units per year, a negligible amount. The erosion hazard near earth is troubled by contradictory information. It is proposed that the meteoroid erosion rate is dominated by sputtering effects, and that the total rate does not far exceed 100 angstrom units per year.

Estimates of penetration and erosion on the lunar surface are in some doubt. Pending the completion of current studies, it is doubtful that the "hazards" exceed the deep space values by more than a factor of two.

THE METEOROID ENVIRONMENT OF PROJECT APOLLO

* * * * * * * *

1. INTRODUCTION

The meteoroid hazard to Project Apollo includes, roughly, any effect on mission success or mission safety owing to collision with uncharted particles. Practically, bodies of "rock" size (a kilogram or more, say) are so infrequent in interplanetary space as to be negligible. The particles of real concern have diameters of several millimeters, or smaller, and weights in the milligram range. The velocities of these particles are characteristic of any bodies in orbit around the sun. They range (at the earth's surface) from 10 to 70 km/second.

Enhanced or reduced hazards occur in regions where either the mass or velocity distribution of the particles is affected. Near a planetary mass, the particle velocities are increased. A very large number of dust particles may be in closed orbits around the earth. On the earth's surface, the atmsophere reduces the hazard to nil; on the moon's surface, it seems likely that quantities of secondary particles of low velocity will be generated by each primary impact. The number of particles is thereby increased.

The hazard to a given space flight may be described by two numbers: firstly, a probability of puncture by larger and less frequent masses; and secondly, a rate of surface erosion by fine dust particles.

The puncture probability is proportional to the "exposure," E, of the spacecraft, defined as the product of its area by the time it spends in a region of homogeneous danger. The units of exposure are chosen as square meters seconds.

The total hazard to a mission is then a sum of hazard rates (per unit exposure) in the various regions, times the exposures in those regions.

Optimum information for Apollo would come from penetration depths measured in recovered capsules. For statistical significance, it is desirable that the total exposure be many times the Apollo exposure.

In this review, we assume the Apollo area to be 70 square meters, and the length of the mission to be 14 days. The exposure is about $10^8 m^2$ sec.

The currently available data is largely in the form of (a) particle fluxes measured as a function of impact momentum or meteor trail brightness, and (b) laboratory penetrations by projectiles an order of magnitude slower than meteoric velocities.

In the following pages the data are reviewed. An attempt is made to produce a best estimate of hazard rates in the various regions, together with an estimate of confidence. Such an appraisal must be in part arbitrary: it is, of course, subject to revision as more experimental facts become available.

2. METEOROIDS: GENERAL

This section is mainly concerned with definitions. For a broader background, the reader is advised to read McKinley[1] or, for a splendid semitechnical account, Watson[2].

A meteoroid is a small object in space. Upon entering the earth's atmosphere, it is consumed, emitting light -- in short, it becomes a meteor. Heavier objects may reach the ground. These may be recovered as meteorites. Lighter objects too faint to be seen may generate enough ionization to be detected by radar as radar meteors. Micrometeoroids are particles sufficiently small that the heat generated in passing through the atmosphere can be radiated away without the consumption of the body. The resulting micrometeorites may be collected (as magnetic dust particles) on earth.

The meteoroids fall into two families characterized by density. The first group, related to the asteroids, has densities from 3 gm/cc (stone) to 8 (iron). Meteors brighter than magnitude -3 are predominantly asteroidal particles.

The second group appears to be cometary debris. Often localized in the orbit of a known comet, these particles are of very low density (perhaps .05 gm/cc in some cases), and are described as "dustballs" or "stoneflakes." These are the fainter visual meteors and the radar meteors. The structure of the smallest cometary particles is unknown. It is difficult to conceive of them as low density.

2.1 Space Distribution: The Showers

Most meteoroids belong to more or less defined associations, i.e. rate fluctuations are large. This is particularly true with dust particles observed by the artificial satellites. Perhaps a quarter of visual meteors belong to major showers, in which fluxes may considerably exceed the average, or sporadic, flux. Five times is characteristic for a strong yearly shower, such as the Perseids, in which the meteoroids are spaced fairly uniformly around their orbit. An increase of a thousand times may occur for periodic showers, whose particles are localized within the orbit. The duration of intense showers can be extremely brief (1-5). The period with which they recur may be many years.

Table I is taken largely from reference (1). It shows the names and dates of major showers, their radiants (apparent origin in the celestial sphere), velocities, and an indication of relative rates expected. It should be noted that there are months - February and September - without major showers.

3. PENETRATION CRITERIA

The numerical quantity of immediate interest to Apollo is the flux of meteoroids capable of penetrating a given structural skin. Since the available information is not in these terms, we must use a "penetration criterion" relating the physical parameters of the meteoroid and target to the depth of penetration. In this section, we select the Ames (Charters and Locke (3)) criterion. This choice is somewhat arbitrary, and should be reconsidered in the light of any new experimental information. As will be seen, however, the differences among the various criteria are not great.

3.1 Hypersonic Impact

The results of a hypersonic impact in a deep target can be briefly described. By "hypersonic" we mean that the particle velocity exceeds the speed of sound in the target. This is about 5 km/sec for most structural metals. Meteoric speeds relative to spacecraft may range from zero to 70 km/second, averaging around thirty.

The experimental data on hypersonic impact (for velocities greater than 10 km/sec) is sparse. The indications are that impact craters are hemispherical, that the total ejected mass is considerably greater than that incident, and that the elastic or plastic constants of the substrate to some degree control crater size. It is not clear what effect the relative densities of particle and substrate have on the process.

3.2 Impact Models

We have studied a number of penetration criteria. These are summarized in Appendix I. The results are as follows: All criteria may be written in terms of the ratio of the ejected mass, M_t, to the incident mass, m. For comparison, they are put in the form:

$$\frac{M_t}{m} = \left(\frac{\rho_p}{\rho_t}\right)^a \left(\frac{v}{v_o}\right)^b \qquad (1)$$

Here a and b are adjustable, v is the velocity of the particle, ρ_p and ρ_p are the densities of particle and target, and v_o is a constant of proportionality dependent on the nature of the target. Experimentalists tend to a v^2 dependence, while theoreticians generally choose v.

In the Ames criterion, the exponent a is +1, i.e. penetration is directly proportional to the ratio of particle density to target density. This seems to be the right way, though the power of the dependence is in some question. Of the other criteria studied, none has a density dependence, save as indicated below (put in the form of equation 1, Bjork[4]'s equation does show an explicit density. However, his computations are only applicable to impacts between equal densities).

The normalizing constant, v_o, is chosen in a number of roughly equivalent ways. It may be related to the speed of sound, as in the Ames criterion. In this form, $v_o = c/6.88$, where c is the speed of sound. It may be related to the strength of the target material, via a "crushing strength," S, (Opik[5]) or the Brinnell Hardness number (Eichelberger and Gehring[6]).

In these cases, the target density always appears in such a way that v_o may be written

$$v_o = \sqrt{\frac{S}{\rho_t}} \qquad (2)$$

That is, the normalizing constant will vary with target density in the same manner as the speed of sound.

3.3 Numerical Comparison - Conclusion

As summarized in Appendix I, these criteria give very similar numerical results in the experimental hypervelocity range. Choosing values suitable for normal impact of aluminum on aluminum, we find that the criteria dependent on the first power of velocity agree within thirty percent or so, and similarly for the v^2 group. The two groups cross at about eleven kilometers per second.

Essentially there is no choice on this basis, and we must wait for good experimental measurements at twenty kilometers per second before the two families can be distinguished.

The Ames criterion is chosen because of the density dependence, which rests on experimental hypersonic impacts on lead targets. It has been widely used in the literature.

The Ames criterion is usually stated as:

$$\frac{p}{d} = 2.28 \left(\frac{\rho_p \quad v}{\rho_t \quad c} \right)^{2/3} \qquad (3)$$

where p is the penetration in a semi-infinite target, and d is the particle diameter. It is assumed that the particle will penetrate a thin wall of thickness 1.5 p.

In the work following, we specialize to aluminum targets. We shall use M.K.S. units. If T is the thickness of material just penetrated, the Ames criterion becomes

$$T^3 = 4.05\ 10^{-13}\ \rho_p\ mv^2 \qquad (4)$$

To convert to other target materials, equation (3) should be used in the following form:

$$\frac{T_1}{T_2} = \left(\frac{\rho_2\ C_2}{\rho_1\ C_1}\right)^{2/3} \qquad (5)$$

where the subscripts 1 and 2 refer to the two materials.

Multiple wall structures may be more or less effective than a single wall of the same total thickness. The appropriate "bumper factor" should be empirically determined and used with equation (5).

4.0 FLUX

Particulate matter in space is counted by a variety of methods appropriate to the abundance of the bodies. As the flux goes down, the exposure of the experiment must become very large. Thus Brown's collection of meteorites[7] had an "exposure" of nearly a million square kilometers for a hundred years ($E = 1.6\ 10^{21}$ meters^2 seconds), while some microphone-type detectors used on sounding rockets have exposures as small as 5 m^2sec and still obtain a reasonable number of counts.

Significant Flux

For an experiment of exposure, E, P impacts will be recorded from a flux N:

$$P = N\ E \gg 1 \qquad (6)$$

For $P \ll 1$, P is the approximate probability of one hit. For any mission, the "significant flux" is easily determined. If the requirement on the hazard is, for instance, .999 chances of no puncture, one must be concerned with the flux for which $P = 10^{-3}$. Thus, for the Apollo mission as a whole ($E_A = 10^8$) the "significant flux" is $10^{-11} m^{-2} sec^{-1}$.

Similarly, for a suited astronaut (exposure, about 2 m^2 for 1 day or about 2 $10^5 m^2$sec) the significant flux is $5\ 10^{-9} m^{-2} sec^{-1}$. Both of these fluxes are small relative to exposures which can be flown today. They fall in the range of the radar meteors, which thus represent the principle source of new flux information on penetration hazards. As of today, the best information still rests on extrapolation from the visible meteors. The radar data is said to be consistent with this approach.

The Flux of Visible Meteors

The flux of visible meteors is "counted" against a magnitude scale. The visual magnitude scale is a logarithmic brightness ranking originally used merely to order stars into six groups by brightness. Today, it has been made more quantitative. The "illuminance," or light flux per unit area (lumens/meters^2) is related as follows to the visual astronomical magnitude, M, of a point source:

$$M = 2.5 \log (e_o/e) \qquad (7)$$

This formula is given in the Handbook of Geophysics[8]. The value of e_o is $1.944\ 10^{-7}$ ft. candles, or $2.094\ 10^{-6}$ meter candles (1 lumen/m^2 = 1 m candle).

Other magnitude scales are defined for photographic plates. The brightness ranks may be quite different for blue-sensitive plates and the human eye. These matters are covered in greater detail in Appendix II.

The cumulative flux, N, of meteors brighter than magnitude M may be expressed by the following equation:

$$N = N_o \, 10^{+.4M} \tag{8}$$

Generally speaking, it is very unlikely that so simple a law is valid. However, it seems to fit the facts reasonably well, and allows ready computation. According to Whipple[9], this may be fitted with the datum of 2.0×10^{8} meteors brighter than the fifth incident on the earth each day. We use a factor of $4.54 \, 10^{19}$ meters^2 second for this exposure. This corresponds roughly to the area of the earth at 100 km altitude. One then obtains for the flux

$$N = 4.4 \, 10^{-14 \, + \, .4M} \; m^{-2} \; sec^{-1} \tag{9}$$

It will be noted that the fifth magnitude flux is $4.4 \, 10^{-12}$, very close to the "significant flux" for the penetration of the Apollo spacecraft. The exact form of the extrapolation[8] is therefore not important. Estimates of this flux will vary more than a factor of two; and, as indicated above, in showers the flux itself may be elevated considerably for weeks at a time. Equation (9) is probably a suitable estimate of penetrating flux both near earth and in cislunar space. We must now go on to the relationship between meteoroid properties and visual magnitude.

Interpretation of Visual Magnitude

The visual magnitude of a meteor is a logarithmic measure of the total luminous flux emitted by the meteor. If it is assumed that the meteoroid is totally consumed, the magnitude is a measure of the initial kinetic energy of the particle.

The luminous efficiency of this process is an unknown. Opik[10] gives a formula "for statistical use" in the analysis of, "dustball type objects, (which appear to be in the majority among visible meteors)," his equation 8-25:

$$\log m = 10.97 - 1.7 \log v - 0.4 M \qquad (10)$$

This may be expressed in M.K.S. units as

$$mv^2 = 3.7 L v^{0.3} 10^{4-0.4M} \qquad (11)$$

where the dimensionless constant L allows one to adjust the luminous efficiency around Opik's preferred value.

Appendix II contains a review of the luminous efficiency problem, including recent experimental determinations[18,21] for solid particles. Since the structure and composition of dustballs are unknown, these determinations are not directly applicable; Opik implies that the luminous efficiency varies differently with velocity for the compact and dustball meteors.

In Appendix II, L is chosen to make the zero magnitude, 30 km/sec meteoroid weigh 2.5 grams. The required value of L is 2.78, with an uncertainty estimated as 3x.

5. THE PENETRATION HAZARD (NEAR EARTH AND DEEP SPACE)

In the above sections, we have chosen a penetration criterion, identified the crucial flux region as that of the visible and radar meteors, written down the distribution law with magnitude, and expressed the relationship between magnitude and kinetic energy of the particle. We can now combine these to compute the likelihood of penetration of a spacecraft of given exposure. We combine equations (4), (9), and (11), obtaining

$$T^3N = 6.6\ 10^{-22}\ v^{.3}\ L\ \rho_p \qquad (12)$$

The value for L was stated above. Since the influence of v is very slight, we choose 30km/sec. A density for meteoroids must be chosen. 500kg/m^3 (0.5g/cc) represents a current view[22]. An uncertainty of 5x brackets most suggested values and allows for alterations in the penetration criterion. With these choices, one obtains

$$T^3N = 2\ 10^{-17}\ \text{(M.K.S. units)} \qquad (13)$$

This result is plotted in Fig. 1. Its validity is expected to cover the penetration range, roughly up to fluxes of 10^{-7}m^{-2}sec^{-1} or so. The expected limits are discussed in Appendix III. Equation (13) should be dependable to a factor of 15x in flux, or about 2.5x in penetration.

The implication of this result for the Apollo mission may be displayed as an illustration. A recent statement of requirements for Apollo (M. Eimer[24]) indicates that the most serious meteoroid problem lies in the service module. The walls can be considered to have 10 m^2 surface area and to comprise two .043cm aluminum sheets separated 2.5 cm.

The equivalent single thickness of aluminum is $8.5\text{x}10^{-4}$ B meters, where B is a "bumper effectiveness" factor which could be as high as two times, but is more likely 1.5x because of structural compromises. We take T = $1.3\text{x}10^{-3}$m. From equation (13), or Fig. 1, the cumulative flux penetrating this is N=$9\text{x}10^{-9}$m^{-2}sec^{-1}

The skin exposure (in a 14-day mission) is E=$1.21\text{x}10^{7}$m^{2}sec, and P = EN = .11. Since P is small, this equals the nominal puncture probability, and the nominal reliability is .90.

6. THE LUNAR SURFACE - SECONDARY EJECTA

The hazard on the lunar surface is complicated by the hypothesized secondary particles arising from primary meteoroid impacts (Gault, Shoemaker, and Moore[11]). These workers estimate that the flux of particles will be raised a factor of 10^3 to 10^4, depending on the nature of the assumptions made as to the lunar surface and the primary flux. These secondaries will be generally slow (averaging under a kilometer per second, probably), only a small fraction having hypersonic velocities. It is, however, estimated that several times the primary mass will leave the moon.

Since penetration has been assumed proportional to kinetic energy, and since the total energy available is conserved, it is conceivable that the actual penetration probabilities are at most doubled.

This is, in fact, our recommendation. We do feel that it is an extremely tenuous recommendation; the fact that a "best estimate" is optimistic is no excuse for ignoring the pessimistic possibilities. Meteoroid penetration measurements should be made on the lunar surface before the Apollo venture.

The penetration hazard on the lunar surface is then expressed as

$$T^3 N = 4\ 10^{-17} \qquad (14)$$

7. OTHER FLUX DATA

We have established above an estimate of the penetration hazard based principally on the properties of the visual meteors. There exists a considerable body of information on the lighter and more frequent meteoroids. Obtained from satellite and other measurements, this information is not directly applicable to penetration estimates, but is essential for a discussion of erosion phenomena.

In this section we discuss the extension of the penetration plot to very much higher fluxes. Only the satellite measurements will be plotted, and the details of these will be retained in Appendix IV. Most of the data has been taken from the review by Alexander, McCracken, Secretan, and Berg[12].

7.1 Direct Measurement of Penetration

At least seven satellites have carried experiments designed to measure the flux of particles penetrating some target. The direct comparison of these requires the assumption of a penetration criterion, since penetration of, for instance, mylar and aluminum, cannot be directly compared until the influence of a target properties is determined. In Fig. 2, the Ames criterion (equation 5) has been used to convert the actual thicknesses to "equivalent aluminum". This may be particularly questionable for the wire-grid targets, which require complete severing of the wire for an indication.

The body of these experiments show "no puncture", suggesting that the fluxes are such that the probability of puncture is 0.5 or less. For simplicity, the points are plotted as (less than) the reciprocal exposure.

The resulting data points are not inconsistent with the penetration curve derived from the meteor data, particularly considering the very poor statistics involved. The extrapolation of this curve is also shown on Fig. 2.

7.2 Acoustic Measurements

A rather different state of affairs is presented by the body of data obtained from microphone measurements. Many satellites have carried sensors sensitive to the momentum of incident particles. Calibration is conventionally performed with low velocity particles, but has been checked with projectiles accelerated to five or six kilometers per second[13]. The calibration constant probably varies a factor of three or four systematically with velocity, since the net momentum transferred to the detector will increase as cratering becomes pronounced.

The acoustic measurements exhibit good statistics and are self-consistent over a large range of fluxes. To plot these, the Ames equation (equation 4) is rewritten

$$T^3 = 4.05\ 10^{-13}\ \rho_p\ v\ (mv) \qquad (15)$$

For these dust particles, it is customary (9) to assume a somewhat higher density and a somewhat lower velocity than for the meteors. We choose a specific gravity of 1 ($10^3 kg/m^3$) and a velocity of $1.8\ 10^4 m/sec$. To plot the data (Appendix IV), we express (15) in terms of c.g.s. momenta, P; the penetration becomes

$$T^3 = 7.3\ 10^{-11}\ P \qquad (16)$$

The results are shown on Fig. 3. It will be noted that, in contrast with the penetration measurements, the acoustic fluxes are well above the low-flux extrapolation. Deep space probes do not show such high fluxes, as indicated by the Pioneer I point on Fig. 3. Preliminary results from Mariner also show low fluxes. Near earth, the discrepancy is noted even in the satellites Samos II and Midas II, which carried acoustic and penetration detectors simultaneously.

The discrepancy is seen more clearly in Fig. 4, which is plotted on a smaller scale. At the upper left are data from the "Venus Flytrap" sounding rocket(15). These are most extreme in all respects. The "Flytrap" collected particles at altitudes between 90 and 160 kilometers. These motes are the smallest and most numerous detected by any technique. Even so, the number of penetrations found in 6 micron mylar film falls below the extrapolated penetration curve. The penetrations are far from hypersonic, the hole diameters being many times the thickness of the film.

As Alexander et al have shown(12), the discrepancy is not apparent on a mass scale, provided that penetrating particles are characterized by diameters approaching the "critical dimensions for fracture" of the detectors, rather than by the Ames penetration criterion.

7.3 Conclusion

It appears in short as though these small particles are incapable of anything like the penetrations which would be inferred from the Ames criterion. It would be very difficult to assign densities and velocities in equation (15) which would fit the facts.

Particular properties which have been suggested for these micrometeoroids are, for instance, that they are in closed orbits around the earth. If the orbits were random, an

average velocity of seven kilometers per second or so would still be observed relative to earth satellites. As suggested above, these particles are unlikely to be less dense than the cometary meteors, and should in fact be more dense.

The notion of special orbits must be eliminated, since comparable results are obtained by equatorial and polar orbiting satellites.

Our current conclusion is to accept the penetration flux of equation (13). At least for deep space, where the acoustic results are in agreement, one can have excellent confidence in this extrapolation. Judging by Fig. 4, the penetrating flux does not exceed $10^{-1} m^{-2} sec^{-1}$, corresponding to the penetration of 6 micron mylar films. This flux rate will be used below to compute an erosion rate.

Near the earth, the situation is more doubtful. Rates predicted by the acoustic measurements are large, and in clear disagreement with other experiments. The penetration flux of equation (13) is retained unchanged, but with somewhat less confidence.

8. EROSION HAZARD

The erosion hazard is involved with the gradual coverage of a spacecraft with small pits. The "coverage time", in which a given area is entirely covered with pits, is the reciprocal of an "erosion rate". For times much shorter than the coverage time, however, the attack will be irregular.

The assumptions made above about the flux of penetrating meteoroids enable the calculation of coverage times. In addition, coverage times will be computed for the near-earth region assuming the acoustic fluxes. The resulting erosion rates far exceed the only measured rates with which we are acquainted.

8.1 Erosion Rates from the Penetrating Flux

We take equation (13) for the flux-penetration relationship.

In accord with the discussion of Section 3, craters of radius T/1.5 will be formed in semi-infinite solids. These craters have areas of $\pi(T/1.5)^2$.

The "coverage rate", in $m^2/m^2 sec$ is obtained by multiplying this area by the flux of the appropriate meteoroids. Thus

$$\pi\ (T/1.5)^2 \cdot N(T) = C \qquad (17)$$

From equation (13), we substitute for T, obtaining

$$C(N) = 10^{-11}\ N^{1/3} \qquad (18)$$

That is, the erosion problem is most serious for high fluxes. Fig. 4 suggests that the penetrating flux, i.e. the flux consistent with equation (13) does not extend above $N = 10^{-1} m^{-2} sec^{-1}$. Substituting in equation (18) we obtain $C\ max = 5\ 10^{-12} sec^{-1}$ for the "coverage rate". The corresponding coverage time is $2\ 10^{11}$ seconds, or approximately six thousand years.

The depth, T, to which this coverage has been attained is about 10 microns. The corresponding erosion rate is 10-20 angstrom units per year.

This value is not badly inconsistent with other estimates. F. Whipple[15], for instance, suggests (from studies of the radio "ages" of meteorites) that an erosion rate of 12 AU/yr makes excellent sense.

To conclude, it appears that at least in deep space, the erosion problem will appear as a coverage of about 10^{-4} of the spacecraft area with small pits, every year.

8.2 Near-Earth Erosion Hazard

Using the acoustic measurements to estimate an erosion hazard near earth, one obtains considerably larger values. As indicated above, we feel that these are not realistic.

From Fig. 3, we obtain a hand fit to the acoustic data. Expressed logarithmically, this is

$$\log N = -20.5 - 4.3 \log T \qquad (19)$$

We now substitute in equation (17). The result is

$$C(N) = 4.5\ 10^{-10}\ N^{.54} \qquad (20)$$

As shown in reference 12, the acoustic measurements are not usually extended above a flux of $10^{3} m^{-2} sec^{-1}$, corresponding to a penetration of about 3 microns.

We substitute the flux value in (20), and obtain a coverage time of almost two years. The inferred erosion rate is about 2000 AU/year.

McKeown & Fox[23] report a measurement of the erosion of a gold surface in low earth orbit (Discoverer 26). The erosion is 0.2±0.1 AU/day, or 70 angstrom units/year. This is attributed entirely to sputtering. The area of the sensor is $10^{-5} m^{2}$. If penetrating fluxes of $10^{3} m^{-2} sec^{-1}$ occur, nearly a thousand micrometeoroid impacts a day would have occurred, whereas the authors identify only one impact in six days.

Our conclusion is that the near-earth erosion rate is less than 100 AU/year, and that the body of this is associated with sputtering, not micrometeoroids.

8.3 Erosion Hazard on the Lunar Surface

Quantitative estimates of the erosion hazard on the lunar surface are extremely difficult to make prior to the release of systematic studies of "ejecta" from primary meteoroid craters.

In view of the lack of knowledge, we suggest planning on an erosion rate double that estimated for deep space, i.e. a coverage of $\sim 10^{-3}$ with pits of radius several microns in a time of one year. In a ten-day mission, the hazard is negligible. As emphasized above, there is no direct support for this estimate. Any experimental evidence would be exceedingly valuable.

9. CONCLUSIONS

An attempt has been made to define the hazards to Project Apollo associated with particulate matter in space. Where information is clearly available to us, it has been used. Where information has been lacking, arbitrary assumptions have been made.

Such a "model" has general usefulness only inasmuch as it is up-to-date, and as its deviation from other proposed models are either justified or explicitly allowed by error estimates.

It is felt that the estimate of penetration hazard is in excellent agreement with other estimates, with the exception that the determination of luminous efficiency may differ. Our present estimate is considered "good".

Further calibration will arise from the "simulated meteor experiments" currently underway with NASA funding. Revision should be undertaken when firm reports are available.

The estimate of erosion hazard in deep space is considered satisfactory, in that the 10-20 angstrom per year figure can not significantly affect spacecraft design. The near-earth erosion estimates are not considered satisfactory, in that the information is contradictory. The possibility of substantially great erosion rates is allowed by the data. The current S-55 satellite (Explorer XVI) should make clear the discrepancy, if any, between acoustic and penetration measurements, and allow a proper calibration.

The estimates of penetration and erosion on the lunar surface must be held in some doubt. The whole problem of ejecta requires (and is currently receiving) careful study. Weighing more than this is the complete lack of empirical information. A single measurement, anywhere in the flux range, for the surface of the moon would enhance the confidence of the whole fabric.

* * * * * *

ACKNOWLEDGEMENTS

We are indebted to a large number of people who have given willingly their time, information, and opinions towards the production of this document.

REFERENCES

1. McKinley, D.W.R., Meteor Science and Engineering, McGraw-Hill, New York, 1961.

2. Watson, F.G., Between the Planets (Revised) Harvard U. Press, Cambridge, Mass., 1956.

3. Charters, A.C., and G.S. Locke, Jr., NACA report A58B26, 1958.

4. Bjork, R.L., Rand Corporation report P 1662.

5. Opik, E.J., Irish Astronomical J., 5, pp. 14-33, 1958.

6. Eichelberger, R.J., and J.W. Gehring, ARS Journal, October 1962, 1583-1591.

7. Brown, H., Jour. Geophys. Res., 65, 6, 1679-83, 1960.

8. Handbook of Geophysics, rev.ed, USAF, Macmillan, NY, 1961.

9. Whipple, F.L. Vistas in Astronautics pp. 115-124 (ed. Morton Alperin, Marvin Stern) Pergamon Press, NY, 1958.

10. Opik, E.J. Physics of Meteor Flight in the Atmosphere, Interscience, New York, 1958.

11. Gault, D.E., E.M. Shoemaker, N.J. Moore, NASA technical note to be published.

12. Alexander, W.M., C.W. McCracken, L. Secretan, and O.E. Berg, Review of Direct Measurements of Interplanetary Dust from Satellites and Probes, presented at a COSPAR meeting, May 1962.

13. Kells, M.C., DD. Keough, Astia document AD 21093.

14. Micrometeorite Collection from a Recoverable Sounding Rocket, ed. R.K. Soberman, G.R.D. research note 71 (Astia AD 272994).

15. Whipple, F.L., Meteoritic Erosion in Space (pre-publication).

16. Levin, B.J., The Physical Theory of Meteors (Ch. I-III) translated, Am. Met. Soc., Astia AD 110091.

17. Millmann & Cook, Astrophysical Journal 130, pp. 648-662 (1959).

18. McCrosky, R.E., and R.K. Soberman, C.R. Research note AFCRL 62-803, July 1962.

19. Hawkins, G.S., Smithsonian Contributions to Astrophysics I, 2, 207-214 (1957).

20. Baker, R.H., Astronomy, Van Nostrand, New York (1950).

21. Cook, Allan F., Luigi G. Jacchia, R.E. McCrosky, Luminous Efficiency of Iron and Stone Meteoroids (pre-publication) G.R.D.

22. F.L. Whipple is currently (January 1963) proposing 0.44 gm/cc.

23. McKeown, Daniel, and Marvin G. Fox, ARS Journal, 954-955, June 1962.

24. Eimer, M., Private Communication.

Table I THE MAJOR METEOR SHOWERS

Shower	Date of Peak Activity	Radiant Coordinates R.A.	Radiant Coordinates Dec.	Duration of Peak, days	Observed Velocity V_o, km/sec	Fractional Rate Increase
Quadrantids	Jan. 3	231°	+50°	0.5	41	6x
Corona Australids	Mar. 16	245	-48	(5)	--	1.5x
Virginids	Mar. 20	190	00	(20)	30	<1.5x
Lyrids	Apr. 21	272	+32	2	48	<1.5x
Eta Aquarids	May 4	336	00	10	64	3x
Arietids (D)	June 7	45	+23	20	39	7x
Zeta Perseids (D)	June 9	62	+24	15	29	5x
Ophuichids	June 20	260	-20	(10)	--	(3x)
Beta Taurids (D)	June 29	87	+20	10	31	3x
Capricornids	July 25	315	-15	(20)	--	3x
Southern Delta Aquarids	July 29	339	-17	15	41	3x
Northern Delta Aquarids	July 29	339	00	20	41	2x
Pisces Aurtralids	July 30	340	-30	(20)	--	3x
Alpha Capricornids	Aug. 1	309	-10	(25)	23	1.5x
Southern Iota Aquarids	Aug. 5	338	-15	(25)	35	2x
Northern Iota Aquarids	Aug. 5	331	-6	(25)	30	2x
Perseids	Aug. 12	46	+58	5	60	6x
Kappa Cygnids	Aug. 20	290	+55	(3)	26	1.5x
Orionids	Oct. 21	95	+15	5	66	3x
Southern Taurids	Nov. 1	52	+14	(45)	29	1.5x
Northern Taurids	Nov. 1	54	+21	(30)	30	<1.5x
Leonids	Nov. 16	152	+22	4	72	1.5x
Phoenicids	Dec. 5	15	-55	(0.5)	(13)	6x
Geminids	Dec. 13	113	+32	6	35	6x
Ursids	Dec. 22	217	+80	2	34	2.5x

APPENDIX I PENETRATION CRITERIA

Several penetration criteria are compared in this appendix. As published, they differ in form and units. In Table I, following, the published formulae are reproduced, with the exception that the symbols are chosen consistently. Thus, M_t, V_t, and R_t are the mass, volume, and radius of the hemispherical hypervelocity crater. The mass and radius of the particle are m and r. The densities of target material and particle are ρ_t and ρ_p. The velocity of the particle is v; the velocity of sound in the target is c. Other parameters are identified in the table.

In the second column, the criteria are reduced to a standard form, as nearly dimensionless as is practicable. The ratio of ejected to incident mass is equated to a product of a density factor and a velocity factor.

$$\frac{M_t}{m} = \left(\frac{\rho_p}{\rho_t}\right)^a \left(\frac{v}{v_o}\right)^b$$

Where the target density does not appear explicitly, the particle density is normalized to the density of aluminum. Otherwise numerical coefficients are lumped in v_o. Hardness or "crushing strength" are lumped with the target density so as to give a normalizing velocity of the form $(\text{strength/density})^{1/2}$.

In the last column, the formulae are evaluated for normal incidence of an aluminum pellet on aluminum. The resulting value for v_o in km/sec is tabulated. The Brinnell Hardness number for aluminum is taken as 170 km/mm^2. This number is the right order of magnitude for a crushing strength as well, and for simplicity, is so used. In comparing the criteria, it will be seen that the v_o for the three square law treatments average 1.3 km/sec ± 30%, and that the three linear treatments average .17 km/sec ± 13%. The cross-over occurs about 11 km/sec.

The choice between the criteria will be made via further experimental work. It should be noted that the Brinnell Hardness number has a rather poor reputation among physical metallurgists; it is easily measured but very difficult to relate to more fundamental material constants. If possible, a more physically meaningful quantity should be used.

APPENDIX I TABLE

Comparison of Penetration Criteria

Source	Form Presented Notes	Standard Form	v_o km/sec
Whipple 1957 (details of article are not used)	$\frac{M_t}{m} = \frac{v^2}{2K}$ K is heat required to raise material to melting point and fuse it. K=1.1 10^6 joules/kg for aluminum.	$\frac{M_t}{m} = \left(\frac{v}{1.48}\right)^2$	1.48
Ames[3]	$\frac{R_t}{2r} = 2.28 \left(\frac{\rho_p \; v}{\rho_t \; c}\right)^{2/3}$	$\frac{M_t}{m} = \left(\frac{\rho_p}{\rho_t}\right)\left(\frac{v}{c/6.88}\right)^2$	.74
Eichelberger & Gehring[6]	$V_t = 4\ 10^{-9}\ (E/B)\ \cos\alpha$ E, kinetic energy B Brinnell Hardness kg/mm^2 B' same, Newton/m^2 α angle of incidence of meteoroid	$\frac{M_t}{m} = \left(\frac{v}{2.26\ (B'/\rho_t)^{1/2}}\right)^2 \cos\alpha$	1.76
McDonnell[16]	$\frac{R_t}{r} = \gamma\left(\frac{\rho_p \; v}{\rho_t \; c}\right)^{1/3}$ $\gamma \sim 4$	$\frac{M_t}{m} = \left(\frac{v}{c/32}\right)$	.16
Bjork[4]	$R_t = 1.09\ (mv)^{1/3}$ cm, gm, km/sec	$\frac{M_t}{m} = \left(\frac{\rho_t}{2.7}\right)\left(\frac{v}{.14}\right)$	.14
Opik[5]	$\frac{M_t}{m} = k\ \frac{v}{(S/\rho_t)^{1/2}}$ $k \sim 4$	$\frac{M_t}{m} = \frac{v}{.25\ (S/\rho_t)^{1/2}}$	.20

APPENDIX II THE PROPERTIES OF VISUAL METEORS

This appendix briefly summarizes the relation between "visible magnitude" and the meteoroid properties of interest, i.e. mass, velocity, and structure. Some preliminary results on simulated meteors will be discussed.

Complete accounts of the theory occur in Opik[10], Levin[16], and throughout the papers of the Harvard Group. Our purpose is not to present a rigorous and complete treatment, but rather to define the problem enough so that the theory and experiment can be compared.

Briefly, it appears that the theoretical treatments are in excellent accord with the facts as far as simulated solid meteors are concerned. Since the nature and composition of dustballs are unknown, there will probably be uncertainty about them for some time.

Magnitude Scales: Photometry

The magnitude scale is very old. Ptolemy's star catalog ranks stars in six "magnitudes" in diminishing order of brightness[20]. In modern times, the scale has been made quantitative and extended in both directions, defining magnitudes above the sixth for stars visible only in the telescope and negative magnitudes for the more brilliant objects (the visual magnitude of the sun is -26.7). Alternate scales (photographic, etc.) are defined for sensors other than the human eye. These scales are made to agree for sources of one spectral type (as, A$_o$ stars, for photographic and visual scales). For this article, we standardize on a conventional photometric scale.[8]

A numerical expression for the "visual astronomical magnitude", M, of a source is

$$M = 2.5 \log e_o/e \qquad \text{II - 1}$$

Magnitude is a measure of the "illuminance", e, of the source, measured in foot candles or lux (meter candles). The constant e_o is the illuminance of a zero magnitude star, 1.944×10^{-7} foot candles or 2.094×10^{-6} lux.

Absolute Visual Magnitude of Meteors

To remove the effects of range and absorption, visual magnitudes are corrected to absolute visual magnitudes. That is, magnitudes are corrected to the value they would have if the meteor were directly overhead at an altitude of 100 kilometers. In this case, the absorption amounts to about 20% of the source flux.

Total Source Flux

If the illuminance at the surface of the earth is e, the total luminous flux Φ, at the source is

$$\Phi = (4\pi R^2 e) \frac{1}{1-\alpha} \qquad \text{II - 2}$$

where R is the range and α the absorption.

Alternately, we may write

$$\Phi = 4\pi R^2 e_o \, 10^{-0.4M} \frac{1}{1-\alpha} \qquad \text{II - 3}$$

$$= \Phi_o \, 10^{-0.4M} \qquad \text{II - 4}$$

where Φ_o is the total luminous flux from a zero magnitude meteor. At an altitude of 100 km, and with an absorption of 20%, $\Phi_o = 3.29 \times 10^5$ lumens.

This corresponds (685 lumens/watt) to 480 watts of monochromatic radiation of wavelength 555 millimicrons. This substantial energy production is related to the instantaneous loss of kinetic energy of the meteor via two factors, one photometric and one physical.

Relative Luminous Efficiency

The "relative luminous efficiency", γ, of any radiation source is its effectiveness in producing visual sensation relative to a source at 555 millimicrons. Typical relative luminous efficiencies are .1355 for black body radiation at 6000°K, and .016 for the iron arc.

Meteor radiation consists of line spectra arising from the decay schemes of excited atoms. The iron lines are generally predominant, other atomic species having much smaller relative efficiencies. The relative luminous efficiency of a meteor can be approximated as

$$\gamma = \gamma_{Fe} \, C_{Fe} \qquad \text{II - 5}$$

where C_{Fe} is the percent of iron in the meteor and γ_{Fe} .016 is the relative luminous efficiency of iron radiation. Properly, equation II-5 should be augmented by similar terms for each element present.

Conversion of Kinetic Energy to Radiation

In addition to the above factors (photometric and chemical), the luminous flux from a meteor is reduced because not all of the meteor's kinetic energy appears as radiation.

The source of the radiant power is the instantaneous loss of kinetic energy, T

$$\dot{T} = \frac{d}{dt} \frac{1}{2} m v^2 \qquad \text{II - 6}$$

Of this, a fraction q appears as radiation; and, as suggested above, a fraction $q \gamma_{Fe} C_{Fe}$ is visually effective. The quantity q is a function of velocity. Opik's analysis suggests an inverse variation with velocity (1/v) for dust balls, and a direct variation (v) for heavy, compact meteoroids. The two species are equivalent near 15 kilometers per second.

Comparison of Theory and Experiment

The comparison of theories and experiment is complicated by this velocity dependence and by a difference in language among the experts.

Opik tabulates (Table LI in reference (10)) his theoretical values of the dimensionless quantity

$$\beta = q \gamma_{Fe} C_{Fe} \qquad \text{II - 7}$$

for both compact and dust ball cases.

R. E. McCrosky and R. K. Soberman have reported results from an artificial meteor experiment. A small (2.2 gm) stainless steel pellet was accelerated by a Trail Blazer II rocket; it re-entered the atmosphere with a velocity of 10 kilometers per second, and was observed by the standard two-camera technique.

In the reduction, a "luminosity coefficient" τ is employed which includes all of the constants mentioned above. It is assumed that $\tau = \tau_0 v$, and τ_0 is tabulated.

In our formalism, we could express the relation between kinetic energy and luminous flux as

$$\dot{T} q \gamma_{Fe} C_{Fe} = \Phi = \Phi_0 10^{-0.4M} \qquad \text{II - 8}$$

The Harvard Group generally uses

$$\dot{T} \tau_0 v = 10^{-0.4 M_{pg}} = 10^{-.72-0.4M} \qquad \text{II - 9}$$

where $M_{pg} = M-1.8$ is the photographic magnitude of the meteor.

Thus, to compare with Opik (II-7), we write

$$\tau_0 = \frac{q \gamma_{Fe} C_{Fe}}{\Phi_0 10^{-.72} v} = \frac{\beta}{\Phi_0 v} 10^{.72} \qquad \text{II - 10}$$

The simulated meteor experiment yields a value

$$\tau_o = 8 \times 10^{-19} \quad \frac{\text{(flux of zero photographic magnitude meteor)}}{\text{grams cm}^3 \text{ sec}^{-4}} \qquad \text{II-11}$$

This is described as a lower limit. The expected range is (6.6-8.6). A possible correction for the chromium content of the pellet would lead to a range of (3, 10) x 10^{-19}.

We insert the value derived above for Φ_o (480 watts), obtaining

$$\frac{\beta}{v} = 7.0 \times 10^{-10} \text{ seconds/cm} \qquad \text{II-12}$$

We evaluate at 15 km/sec and obtain the following experimental value, recalling that it is quoted as a lower limit and has an uncertainty something near two times associated with it.

$$\text{Iron} \quad \beta = 10^{-3} \qquad \text{(Experimental)} \qquad \text{II - 13}$$

Opik, in his Table LI[10], does not distinguish between iron and stone meteoroids, i.e. no composition dependence is implied. For velocities of 14.8 km/sec the values of β are as follows for the "dilute coma" and "compact coma" (comparable with McCrosky) cases:

$$\beta \text{ dilute} = 1.00 \times 10^{-3}$$
$$\beta \text{ compact} = 1.10 \times 10^{-3} \qquad \text{(Theory)} \qquad \text{II - 14}$$

The agreement may be mildly described as excellent.

Additional Information

A very detailed analysis of three photographic meteors has been made by Cook, Jacchia, and McCrosky.[21] By careful study, they estimate the radius of an iron meteor ($0.5 \leqslant r \leqslant 0.9$ cm) and derive a mass and hence a luminosity coefficient. Choosing r = 0.7 cm, they obtain

$$\tau_o = 2 \times 10^{-18} \text{ (units as above) range (1 to 6)} \qquad \text{II - 15}$$

or

$$\frac{\beta}{v} = 1.8 \times 10^{-9} \text{ seconds/cm}$$

$$\beta = 2.7 \times 10^{-3} \text{ at 15 km/second} \qquad \text{(Experimental)} \qquad \text{II - 16}$$

The uncertainty here is presumably rather more than two times. The agreement is good.

Luminous Efficiency of Dust Balls - Conclusions

As noted in the text, Opik's formula "for statistical use" with dust balls has been employed. His luminous efficiency is, however, divided by a constant L.

$$\beta = \frac{10^{-3}}{L} \quad (v = 15 \text{ km/second}) \qquad \text{III - 17}$$

As stated above, however, luminous efficiency should have the form

$$\beta = q \, \gamma_{Fe} \, C_{Fe} \qquad \text{II - 7}$$

This has the authority of the Harvard Group and Levin, the composition of dust balls is unknown, but may approach meteoric stone (15% iron). If we accept $\beta = .5\text{-}5 \times 10^{-3}$ as the range allowed by the experimental results for pure iron, with a probable value near one or two, good dust ball values for L would range from 1 to 10, 3x being a logarithmic mean. The chosen value, 2.78, has the significant advantage of fitting a previously established penetration hazard model. There seems to be no reason to abandon it.

Further work on the simulated meteor program will tie down the value of τ and its variation with velocity and composition. Little direct information on dust balls will be obtained, since the nature of these objects is so little understood.

APPENDIX III CONFIDENCE IN EQUATION (13)

We wish to estimate the confidence in equation (13) as far as the significant flux for the Apollo spacecraft is concerned ($10^{-11} m^{-2} sec^{-1}$). Equation (13) may be rewritten in the following way, now retaining all the adjustments:

$$T^3 N = 6.6\ 10^{-22} v^{0.3} L \rho_p \cdot (N_o / 2\ 10^8)(11/v)^{\delta}\ m/sec$$

To adjust the flux, the fifth magnitude value, N_o, appears. To account for a possible momentum dependence of penetration, the last factor is included. The exponent $\delta = 1$ in that case, 0 otherwise. If the density dependence of the Ames criterion is false, ρ_p should be set to the aluminum value, $2.7\ 10^3 kg/m3$. Formally, the slope of the flux-magnitude plot should also appear. For discussing the penetration hazard, we will lump its uncertainty with that in N_o.

Preliminary estimates suggest that L may vary by a factor of three. The density may vary perhaps five times. N_o may be uncertain by a factor of about four. In the case of momentum dependent penetration, the factor (11/v) will be one third for the average meteoroid. The logarithmic errors are then, respectively, .5, .7, .6, .5. The approximate expected deviation is estimated by taking the root mean square of the logarithmic deviations.

$$\sqrt{.25 + .49 + .36 + .25} = 1.16$$

or about 15x in flux. This amounts to 2.5x in penetration.

APPENDIX IV FLUX CHART DATA

The data employed here are taken largely from reference (12), an excellent and complete review. As shown in the text, the acoustic measurements are plotted using the following equation:

$$T^3 = 7.3\ 10^{-11}\ P$$

The penetration in meters is given by T, while P is the momentum sensitivity of the microphone in dyne-seconds.

In plotting the penetration measurements, the "characteristic dimensions for penetration" must be converted to equivalent aluminum thicknesses. The choice of the Ames criterion requires, then, scaling as the two-thirds root of the product of target density and velocity of sound. When more data is available, the smoothness of such a plot will be helpful in choosing a proper penetration law. The few penetrations recorded here would plot more smoothly without the transformation.

In particular, the transformation for mylar films may be in question, since the film properties have been, in part, estimated.

The preliminary results from the "Venus Flytrap" sounding rocket[14] give a flux of 300 per meter^{2}sec of particles having diameters above 3 microns. The flux varies as the inverse 1.2 power of diameter in the flux range of 3×10^2 to about $1.6\times10^4 m^{-2}sec^{-1}$.

Using the Ames criterion, one obtains from these facts

$$T\ N^{.833} = 1.18\times10^{-3} \left(\frac{\rho_p}{\rho_t}\ \frac{v}{c}\right)^{2/3} \qquad \text{(M.K.S.)}$$

As for the acoustic measurements, ρ_p is taken as 1 gm/cc. The particle velocity is assumed 10 kilometers/second, giving

$$T\ N^{.833} = .97\times10^{-3}$$

Conversion to Equivalent Aluminum

$$Te = T \left(\frac{\rho\ C}{\rho_e\ C_e}\right)^{2/3} = T \times A$$

Material	ρ gm/cc	C km/sec	A
Pyrex	2.8	5-6 (?)	.93
Mylar	1.4	1.4*	3.7
Magnesium	1.7	4.6	1.5
Stainless Steel 304	7	5 (?)	.54
Copper	8.9	3.6	.58
Aluminum	2.7	5.1	-

*Computed from Tensile elastic modulus 550,000 psi

APPENDIX IV

Table 1 Penetration Measurements

Space Craft	Material	Penetration (m)	Equivalent Aluminum* (m)	Exposure (m^2sec)	Impacts	Flux ($m^{-2}sec^{-1}$)
Vanguard III	pyrex	$3\ 10^{-4}$	$3.2\ 10^{-4}$	7 10	0	$<1.4\ 10^{-2}$
	pyrex	$3\ 10^{-4}$	$3.2\ 10^{-4}$	$1.4\ 10^{2}$	0	$<7\ 10^{-3}$
	mylar	$6\ 10^{-6}$	$1.6\ 10^{-6}$	8.7 10	0	$<1.1\ 10^{-2}$
	magnesium	$6.5\ 10^{-4}$	$4.3\ 10^{-4}$	$7.2\ 10^{5}$	0	$<1.4\ 10^{-6}$
Explorer VII	mylar	$6\ 10^{-6}$	$1.6\ 10^{-6}$	3.9 10	1	$2.5\ 10^{-2}$
Explorer XIII	stainless	$7.5\ 10^{-5}$	$1.4\ 10^{-4}$	$3.4\ 10^{4}$	0	$<3\ 10^{-5}$
	stainless	$1.5\ 10^{-4}$	$2.8\ 10^{-4}$	$8.5\ 10^{3}$	0	$<1.2\ 10^{-4}$
	"wire" Cu & enamel	$7.5\ 10^{-5}$	$1.3\ 10^{-4}$	$1.7\ 10^{3}$	0	$<6\ 10^{-4}$
	"wire" Cu & enamel	$5\ 10^{-5}$	$8.6\ 10^{-5}$	$7.7\ 10^{2}$	0	$<1.3\ 10^{-3}$
Explorer I	"wire" Cu & enamel	$1.7\ 10^{-5}$	$3\ 10^{-5}$	$3.6\ 10^{3}$	0	$<2.8\ 10^{-4}$
Explorer II	"wire" Cu & enamel	$1.7\ 10^{-5}$	$3\ 10^{-5}$	$2.4\ 10^{2}$	2	$8.3\ 10^{-3}$
		Counts Received During a Shower				
Midas II	"wire" Cu & enamel	$2.0\ 10^{-5}$	$3.5\ 10^{-5}$	$2.\ 10^{3}$	0	$<5\ 10^{-4}$
Samos II	"wire" Cu & enamel	$2\ 10^{-5}$	$3.5\ 10^{-5}$	$1.1\ 10^{4}$	8	$7\ 10^{-4}$
Venus Flytrap[14]	mylar	$6\ 10^{-6}$	$1.6\ 10^{-6}$	5.7x10	3	$5\ 10^{-2}$

* See text.

Appendix IV

Table 2 ACOUSTIC MEASUREMENTS

Spacecraft	Sensitivity P, dyne-sec	Observed Flux ($m^{-2}sec^{-1}$)	Penetration Inferred (m)
Explorer VIII	$2.5\ 10^{-3}$	$1.5\ 10^{-2}$	$5.6\ 10^{-5}$
	$2.5\ 10^{-2}$	$3.1\ 10^{-4}$	$1.3\ 10^{-4}$
	$2.5\ 10^{-1}$	$5.6\ 10^{-6}$	$2.6\ 10^{-4}$
		less than 2 impacts	
Vanguard III	10^{-2}	$1.3\ 10^{-3}$	$9\ 10^{-5}$
Pioneer I	$1.5\ 10^{-4}$	$4\ 10^{-3}$	$2.2\ 10^{-5}$
Explorer I	$2.5\ 10^{-3}$	$8.4\ 10^{-3}$	$5.6\ 10^{-5}$
Ranger I	$3\ 10^{-5}$	7.3	$1.3\ 10^{-5}$
Midas II	$3\ 10^{-4}$	$2.5\ 10^{-1}$	$2.8\ 10^{-5}$
Samos II	$3\ 10^{-4}$	$3.4\ 10^{-1}$	$2.8\ 10^{-5}$
SLV	$9\ 10^{-3}$	$1.3\ 10^{-2}$	$8.7\ 10^{-5}$
		Additional	
Venus Fly Trap		(see text of Appendix IV)	

FIG. 1

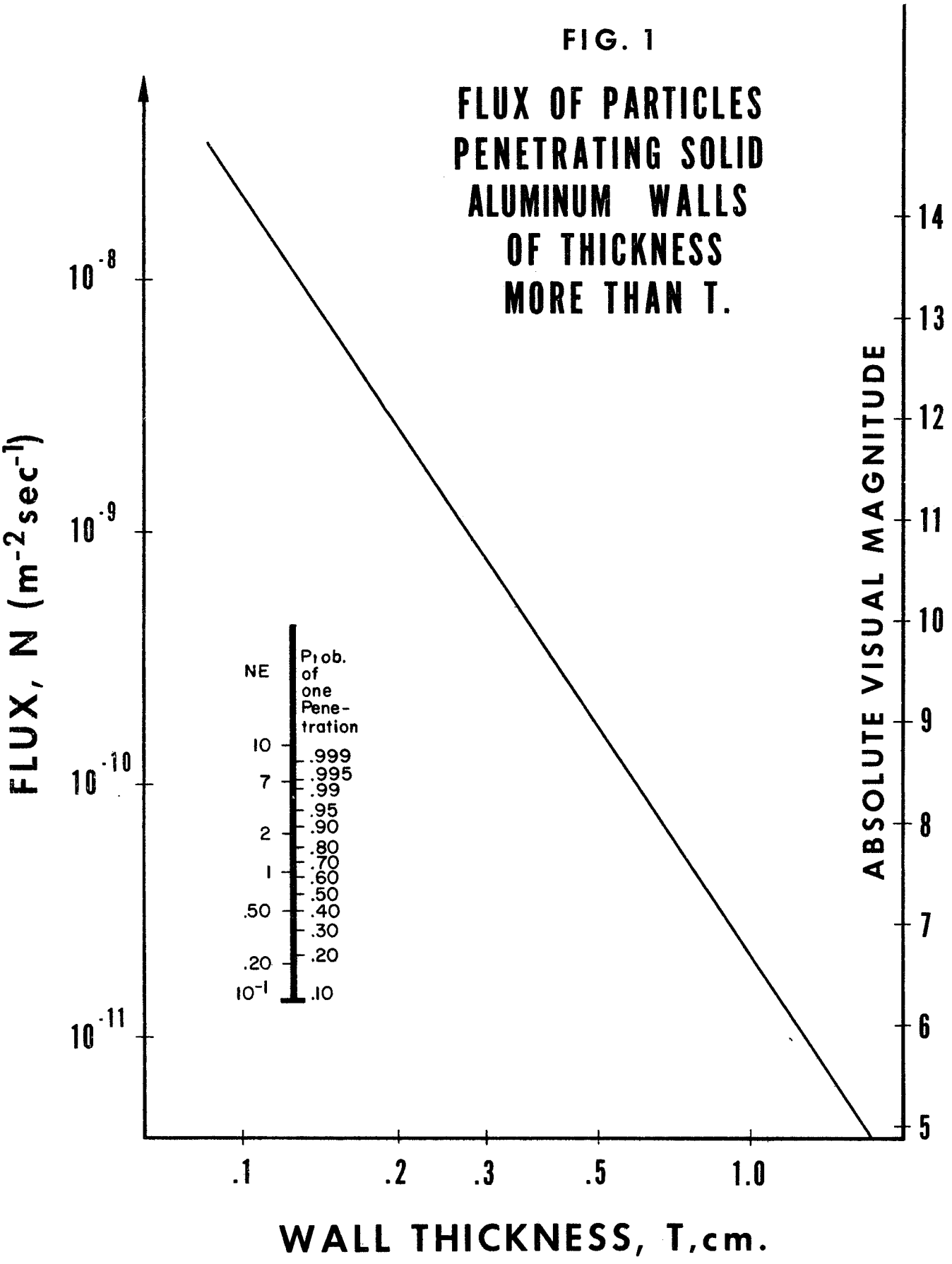
FLUX OF PARTICLES PENETRATING SOLID ALUMINUM WALLS OF THICKNESS MORE THAN T.
FLUX, N ($m^{-2}sec^{-1}$)
10^{-8}
10^{-9}
10^{-10}
10^{-11}
NE
Prob. of one Penetration
10
7
2
1
.50
.20
10^{-1}
.999
.995
.99
.95
.90
.80
.70
.60
.50
.40
.30
.20
.10
.1
.2
.3
.5
1.0
WALL THICKNESS, T, cm.
ABSOLUTE VISUAL MAGNITUDE
14
13
12
11
10
9
8
7
6
5

FIG 2

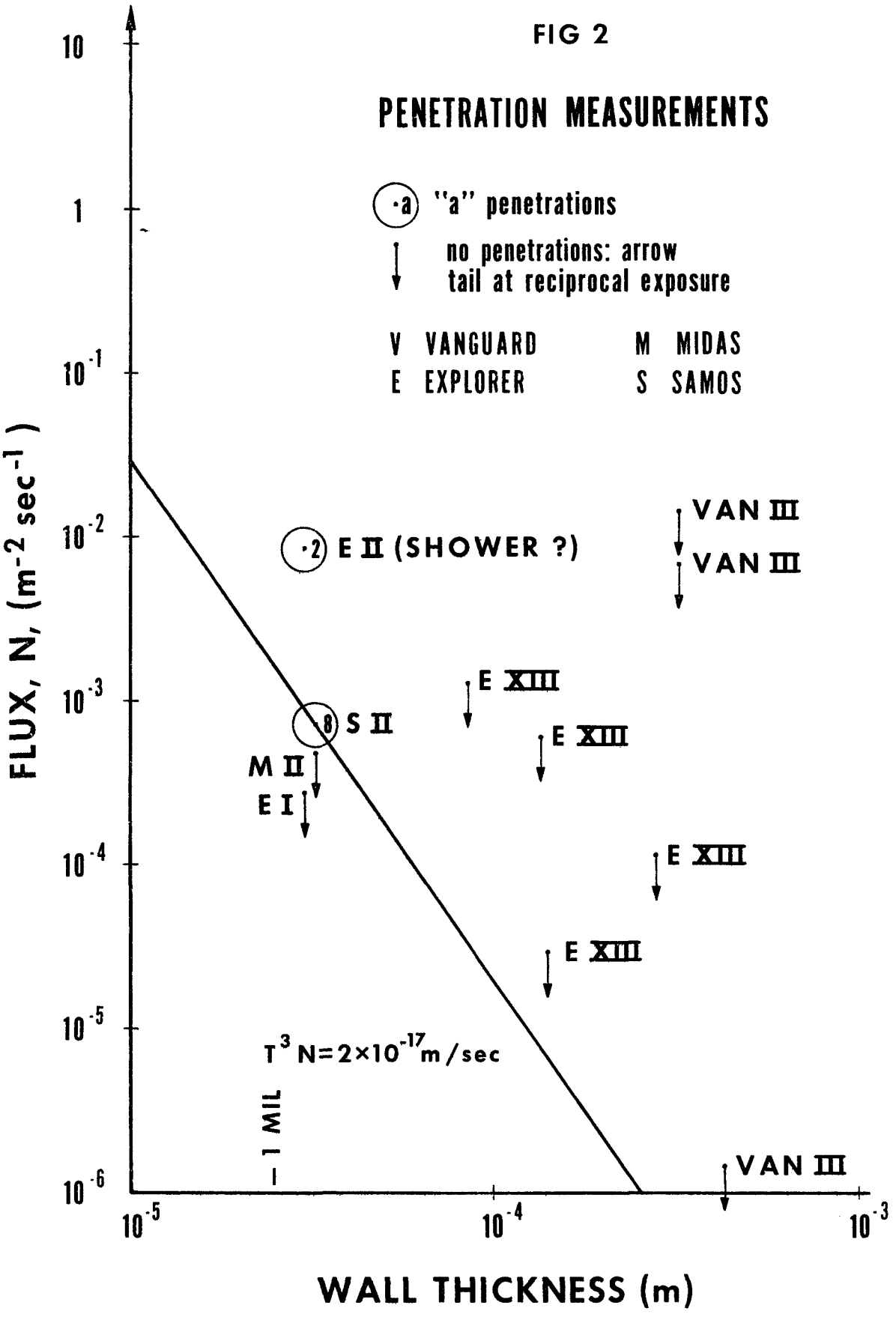
PENETRATION MEASUREMENTS
·a "a" penetrations
no penetrations: arrow tail at reciprocal exposure
V VANGUARD
E EXPLORER
M MIDAS
S SAMOS
FLUX, N, (m⁻² sec⁻¹)
10
1
10⁻¹
10⁻²
10⁻³
10⁻⁴
10⁻⁵
10⁻⁶
·2 E II (SHOWER ?)
VAN III
VAN III
E XIII
E XIII
·8 S II
M II
E I
E XIII
E XIII
T³ N=2×10⁻¹⁷ m/sec
1 MIL
VAN III
10⁻⁵
10⁻⁴
10⁻³
WALL THICKNESS (m)

FIG 3

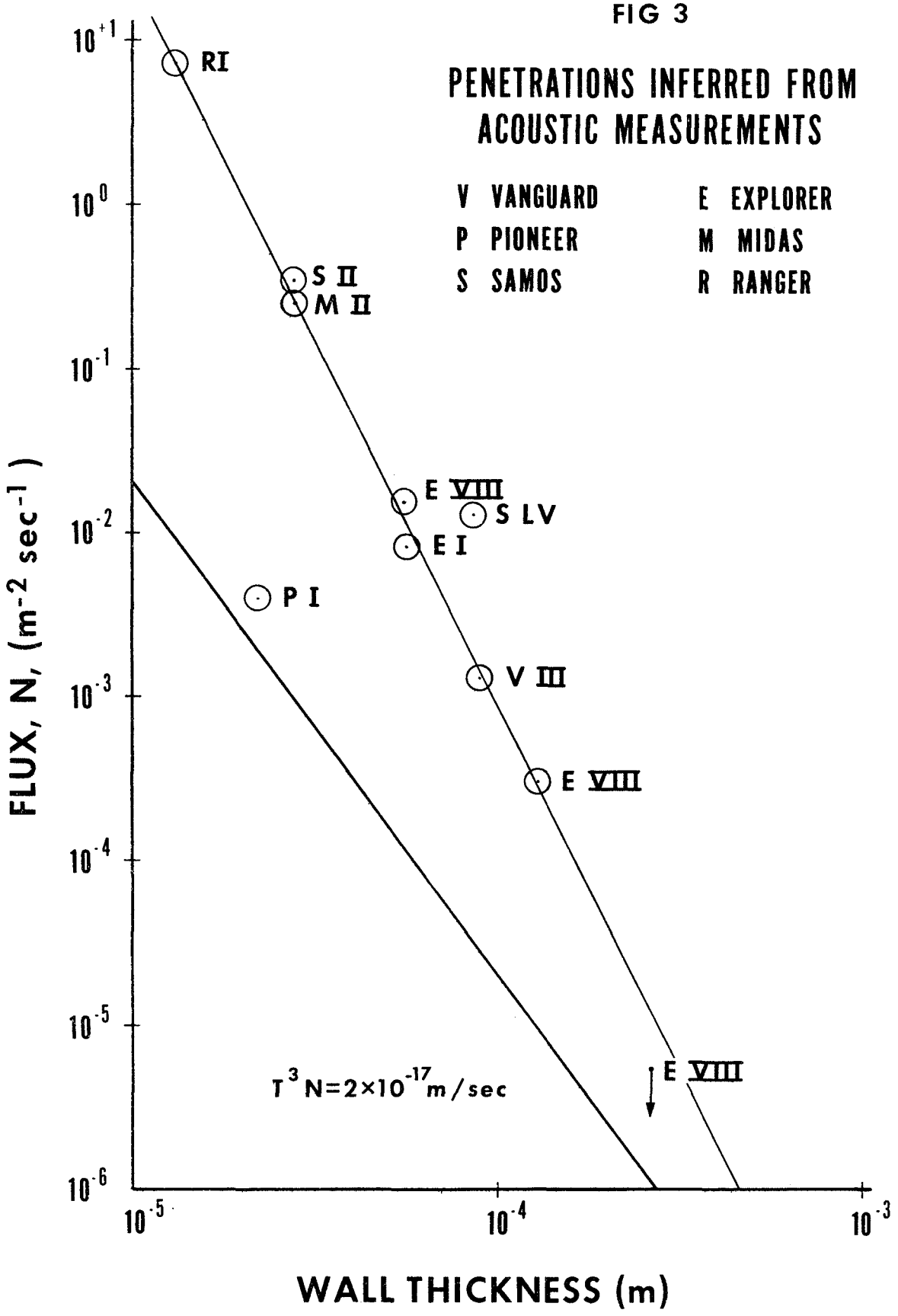
PENETRATIONS INFERRED FROM ACOUSTIC MEASUREMENTS
V VANGUARD
P PIONEER
S SAMOS
E EXPLORER
M MIDAS
R RANGER
RI
S II
M II
E VIII
S LV
E I
P I
V III
E VIII
E VIII
$T^3N=2\times10^{-17}$ m/sec
FLUX, N, (m^{-2} sec^{-1})
WALL THICKNESS (m)
10^{+1}
10^{0}
10^{-1}
10^{-2}
10^{-3}
10^{-4}
10^{-5}
10^{-6}
10^{-5}
10^{-4}
10^{-3}

FIG 4

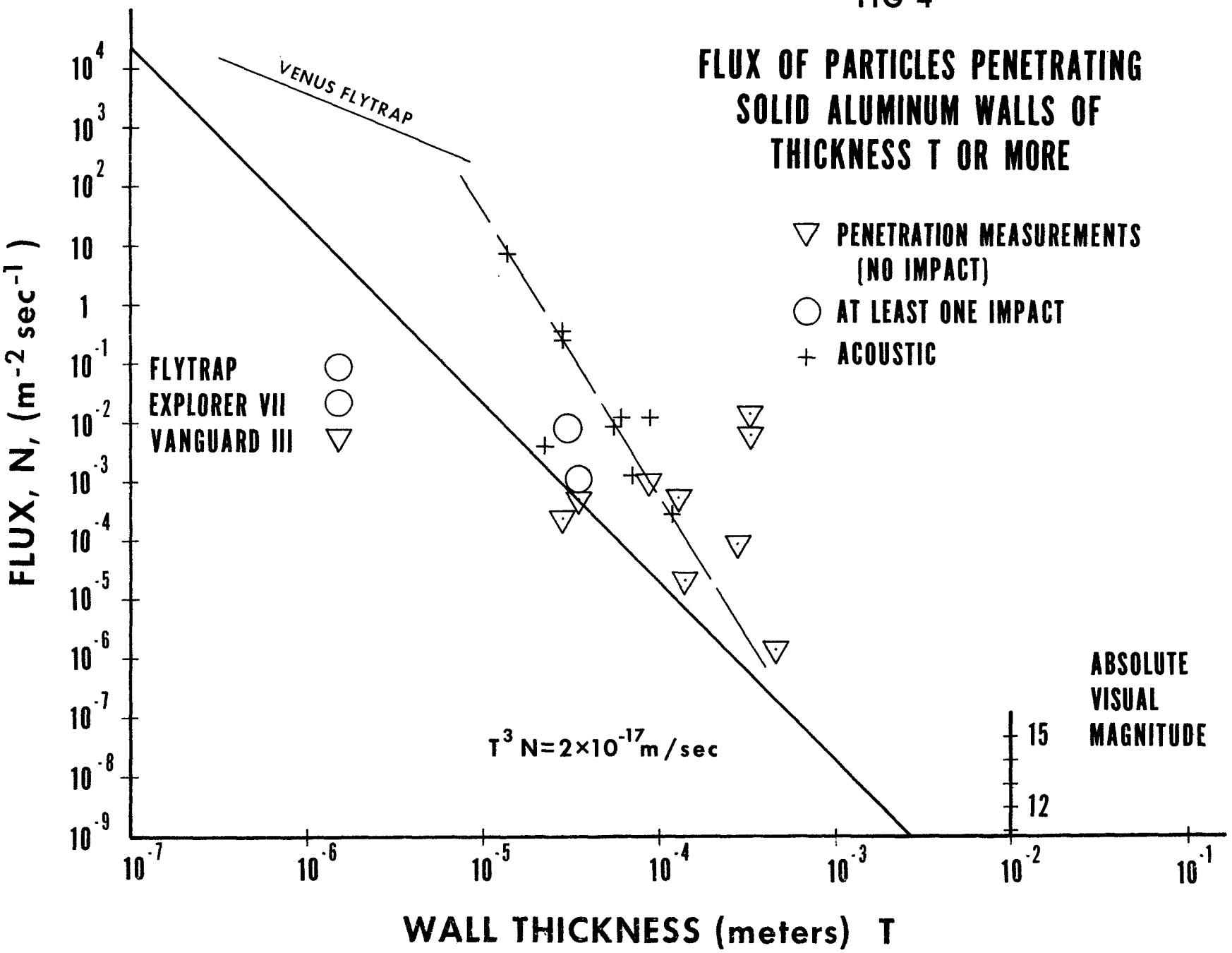
FLUX OF PARTICLES PENETRATING SOLID ALUMINUM WALLS OF THICKNESS T OR MORE
PENETRATION MEASUREMENTS (NO IMPACT)
AT LEAST ONE IMPACT
ACOUSTIC
VENUS FLYTRAP
FLYTRAP
EXPLORER VII
VANGUARD III
$T^3 N = 2 \times 10^{-17}$ m/sec
ABSOLUTE VISUAL MAGNITUDE
15
12
FLUX, N, (m^{-2} sec^{-1})
10^{4} 10^{3} 10^{2} 10 1 10^{-1} 10^{-2} 10^{-3} 10^{-4} 10^{-5} 10^{-6} 10^{-7} 10^{-8} 10^{-9}
10^{-7} 10^{-6} 10^{-5} 10^{-4} 10^{-3} 10^{-2} 10^{-1}
WALL THICKNESS (meters) T


BELLCOMM
BELL
SYSTEM
INC.